

Optical design of GaN resonant cavity LEDs emitting at 510nm for use in plastic optical fibre applications.

Alan Shaw^{*}, John F. Donegan, James G. Lunney, Louise Bradley
Semiconductor Photonics Group, Physics Department, Trinity College Dublin

ABSTRACT

The optimized optical design of GaN resonant cavity light emitting diodes (RCLEDs) emitting at 510nm for maximum extraction efficiency into numerical apertures (NAs) of 1.0 (total emission) and 0.5 (typical plastic optical fiber NA) are determined using a modeling tool based on the simulation of dipole emission in a multilayer structure. The optimization is performed for a metal-AlGaIn/GaN DBR cavity structure as functions of the aluminum fraction in the DBR and the internal quantum well (QW) emission linewidth. The optimum number of DBR pairs is shown to depend on both these parameters together and the emission NA, and varies between 3 and 14. The maximum calculated extraction efficiency for a metal-AlN/GaN cavity structure, assuming a QW emission linewidth of 30nm, is 0.18 (0.055) into an emission NA of 1.0 (0.5). The position of the QW relative to the metal mirror is shown to be the crucial device parameter in determining the extraction efficiency of the RCLED. Simulations show farfield measurements should provide information on the position of the QWs in the cavity. The reduction in the spectral emission linewidth of the RCLED due to the cavity is also modeled.

Keywords: Resonant cavity light emitting diode, Gallium Nitride, plastic optical fibre

1. INTRODUCTION

The capacity of RCLEDs to produce higher spectral purity and increased directionality of emission compared to conventional LEDs was first realised by Schubert and co-workers in GaAs based devices emitting at 860nm¹. These effects are due to the modification of the spontaneous emission process resulting from the coupling of emission from the active layer of the RCLED to the modes of the cavity. This modification of the spontaneous emission process can also be used to improve the extraction efficiency of LEDs by increasing emission at internal angles less than the critical angle for light to escape from the device, as first demonstrated by DeNeve². The combination of the RCLEDs enhanced extraction efficiency through a single surface and enhanced directionality of emission translates into improved radiance, defined as optical power per unit solid angle and unit emitting area, compared to conventional LEDs. The high radiance of RCLEDs is important in applications where the emission has to be coupled into an optical system of a given numerical aperture (NA), for example optical fibres, optical scanners, printers, optical interconnects and certain display applications. One particular application where RCLEDs have shown considerable promise is as sources for plastic optical fibre (POF) based networks, where the large core diameter of POF and relatively low bandwidth (<1Ghz) requirements for such applications are compatible with current RCLED technology. Red AlGaInP-based RCLEDs whose emission wavelength is matched to the POF transmission window at 650nm have demonstrated impressive performance and are ready for large-scale production³. Additional POF transmission windows exist at 510nm and 570nm. These wavelengths are accessible using III-V nitride semiconductors, materials whose properties are less temperature dependent than the AlGaInP materials used for emission in the red. Therefore these materials hold the potential for a reduced temperature sensitivity of device performance as required for POF applications in automotive and avionic environments.

Blue and Violet GaN RCLEDs have already been demonstrated showing clear cavity effects in the emission spectrum and directionality of emission^{4,5}. These structures were designed to achieve high Q cavities suitable for vertical cavity surface emitting laser (VCSEL) devices, but no effort was made to optimize the cavity design for maximum light extraction efficiency. Determining the optimum design and performance of GaN resonant cavity light emitting diodes (RCLEDs) is essential to assessing the potential and limitations of these devices in practical applications. In this paper, a model capable of the exact simulation of dipole emission in an arbitrary planar structure is employed to investigate

^{*} ajshaw@tcd.ie; phone 353 1 6082881; fax 353 1 6082680; Physics Department, Trinity College Dublin, Dublin 2, Ireland.

optical design considerations of a GaN/AlGaIn/InGaIn resonant cavity LED emitting at 510nm. The optimum design for maximum extraction efficiency into air and into a fiber with a typical POF NA of 0.5 is presented, and the key design parameters and optimized device performance are discussed.

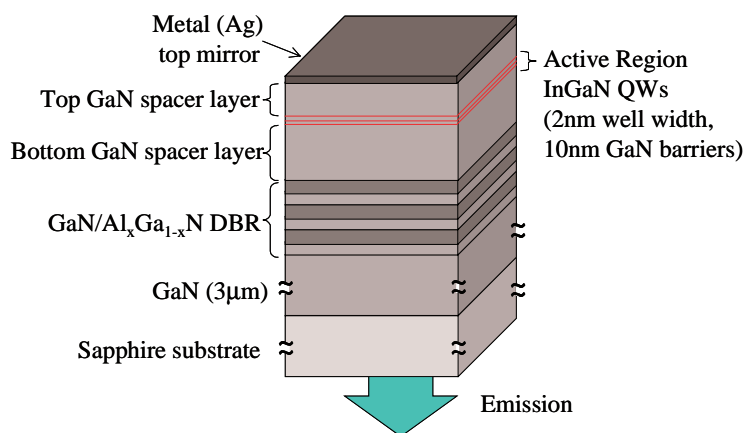


Figure 1. Schematic diagram of substrate emitting, hybrid metal-DBR GaN RCLED.

The generic GaN RCLED structure investigated consists of a substrate-emitting device with a hybrid cavity formed from a metal top mirror and an AlGaIn/GaN DBR bottom mirror. The choice of a metal top mirror for our cavity, while not offering as high a reflectivity as a high refractive index contrast dielectric DBR (e.g. $\text{HfO}_2/\text{SiO}_2$), minimizes the effective cavity length by eliminating the significant penetration depth present in DBR mirrors while still maintaining a high reflectivity. Since the cavity length plays a determining role in the extraction efficiency of RCLEDs (see section 2.1) the hybrid metal-DBR cavity structure is deemed optimal for RCLEDs⁶, as confirmed by extensive analysis and measurements on RCLEDs emitting at 980nm. This structure also has the benefit of the bottom mirror being compatible with epitaxial growth techniques, while the top metal mirror can act as an electrical contact. The impact of the relatively small refractive index variation of AlGaIn with Al fraction compared to AlGaAs on the properties of AlGaIn/GaN distributed Bragg reflectors (DBRs) has important implications for the design of these devices.

2. THEORY AND MODEL

2.1 General theory of RCLEDs

The main focus of this paper is the modeling and optimization of the extraction efficiency of GaN RCLEDs. In this section the principle by which the angular redistribution of emission that occurs in a cavity due to interference effects can be exploited to enhance the extraction efficiency in RCLEDs, is introduced. An extensive treatment of the theory of light extraction efficiency in planar cavity structures is contained in two seminal papers by Benisty^{7,8}.

In order to demonstrate the ability of a cavity to modify the angular distribution of emission, the emission from a source in a planar cavity (Fabry-Perot cavity) is calculated using a classical multiple beam interference approach. A source emitting at vacuum wavelength λ , positioned in a cavity of thickness L and refractive index n , at a distance z_1 from the bottom mirror is considered (see Figure 2). The top (bottom) mirror reflectivity and transmission are denoted $R_1=r_1^2$ ($R_2=r_2^2$) and $T_1=t_1^2$ ($T_2=t_2^2$) respectively, where r_1 and r_2 (t_1 and t_2) are electric field amplitude reflection (transmission) coefficients. The source emits rays that interfere before being collected in the farfield above the cavity. The summation of two series of waves one emitted at θ and the other emitted at $\pi-\theta$, gives the following expression for the farfield intensity E^2 corresponding to an internal angle θ

$$|E|^2 = |E_0|^2 \times \frac{T_1}{|1 - r_1 r_2 e^{2i\theta}|^2} \times |1 + r_2 e^{2i\theta}|^2 \quad (1)$$

where $\phi' = kz_1 \cos \theta$, $\phi = kL \cos \theta$, with $k = 2\pi n / \lambda$, and E_0 is the radiated far-field from the source at an angle θ in the absence of any mirror.

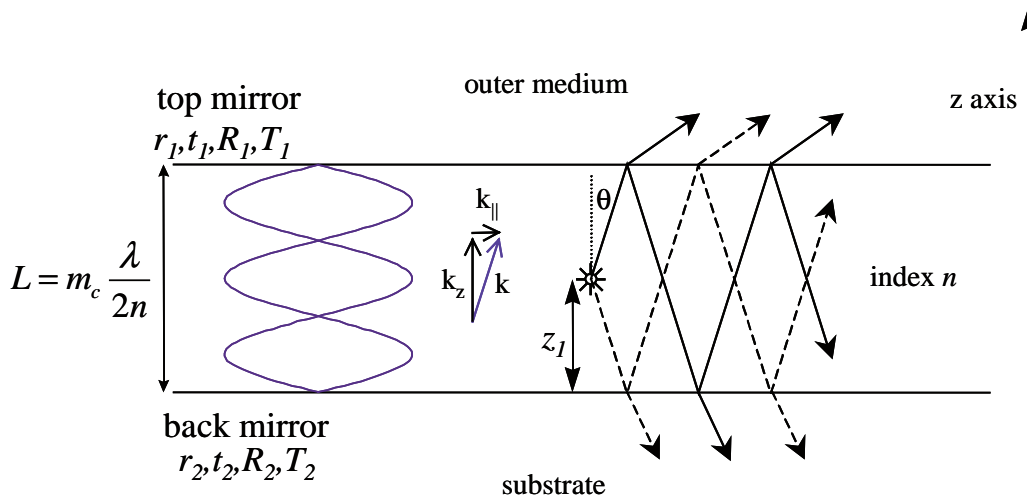


Figure 2. Schematic representation of planar cavity of index n and length L , with an internal source emitting two series of waves.

The final term $|1 + r_2 e^{2i\phi'}|^2$ in (1) is called the antinode factor ζ , and corresponds to the enhancement of the upward radiated farfield in the presence of a single bottom mirror. The periodic variation of ζ with ϕ , corresponds to constructive and destructive interference between the rays emitted from the source at θ and those emitted at $\pi - \theta$, in the presence of a single bottom mirror. To maximize the farfield intensity at the angle θ , for the source wavelength λ , we require $2\phi' (=2kz_1 \cos \theta) = 2m\pi$ where m is a (half) integer for $(-)$ $+r_2$. To satisfy this condition at $\theta=0$, we require $kz_1 = m\pi$ or $z_1 = m\pi/k = m(\lambda/2n)$. Since the only dependence of the farfield intensity from the cavity, given by (1), on the source position z_1 , is contained in ζ , the source should be positioned at an integer number of half wavelengths from the bottom mirror for maximum on axis ($\theta=0$) emission (for $+r_2$). This corresponds to the positioning of the source at an antinode of the cavity mode.

The second term in (1), $\frac{T_1}{|1 - r_1 r_2 e^{2i\phi}|^2}$ is known as the Airy factor and accounts for the cavity mode structure. It reproduces the intrinsic enhancement/inhibition of each mode (i.e. each wavelength, angle pair) by the cavity. The Airy function is a maximum for $\phi (=kL \cos \theta) = m\pi$, with the width of the resonance around the maximum value determined by the mirror reflectivities. This resonance condition determines the wavelength-angle pairs that represent cavity modes. For a fixed emission wavelength, k is constant and ϕ can vary from 0 at $\theta = \pi/2$ to kL at $\theta=0$, satisfying the resonance condition of the cavity at angles θ such that $k \cos \theta = m\pi/L$. Therefore the cavity order m_c , defined as the number of cavity resonances, is given by $m_c = \text{integer}[kL/\pi]$ (where $\text{integer}[x]$ means the value of x rounded down to the nearest integer). While the cavity length for a cavity with a resonant mode at $\theta=0$, is given by $L = m_c \lambda / 2n$.

The farfield emission for a source positioned at the center of a $m_c=6$ cavity (r_1, r_2 both positive), together with the Airy and antinode functions are shown in Figure 3. The six modes of the cavity are clearly visible in the Airy function, while the antinode factor shows that the positioning of the emitter at the center of the cavity results in emission only coupling to every second cavity mode. Depending on the emitter position in the cavity emission into the even or odd cavity modes can be equally or unequally favoured. Figure 3(b) shows the capability of the cavity to radically alter the emission pattern of an isotropic source placed in a cavity. This effect can obviously be used to alter the emission profile

from microcavity LED structures, however the angular redistribution of emission inside the cavity can also be used to improve the extraction efficiency of LEDs.

The ability of a microcavity to enhance the extraction efficiency is best demonstrated using a k -space plot of the cavity modes and Airy function, a scheme developed by Benisty et al.⁷. The case of a monochromatic source is again considered, but in order to simplify the discussion we initially assume that ζ is the same for all modes in the cavity (this corresponds to a situation where the source is distributed throughout the cavity). In this situation the angular distribution of emission is determined solely by the Airy function, whose resonances are periodic in $k_z = k \cos \theta$. The intersection of

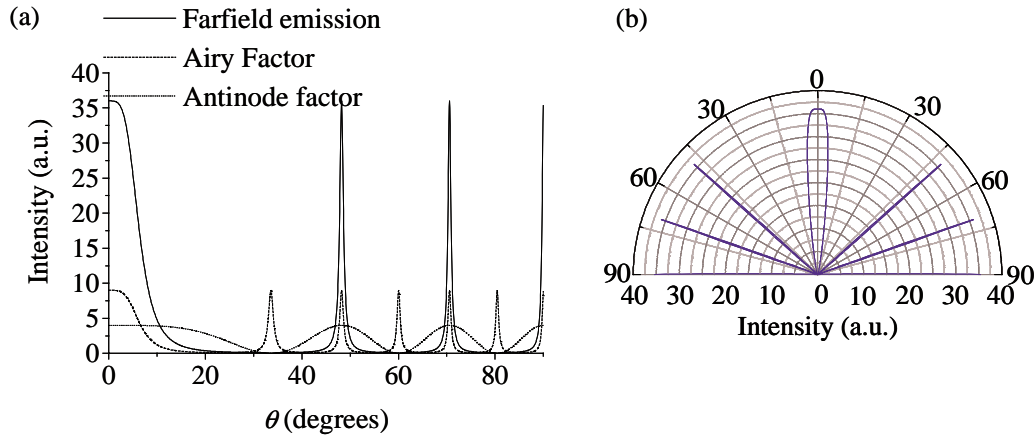


Figure 3 (a) Emission profile of an isotropic source (monochromatic emission at wavelength λ) positioned at the centre of an $m_c=6$ ($L=3\lambda/n$), for $r_2=+1, r_1=+0.8$, and $T_j=0.36$, (b) same farfield emission profile on a polar plot.

the quarter circle of radius k , with the horizontal lines for each resonant $k_z = m\pi/L$ determines the angles of the resonant cavity modes. It can be shown that the total emission in a cone between two angles θ_1 and θ_2 , accounting for the variation in solid angle with θ , is given to within a constant factor by the integration of the Airy function in Figure 4 between $k_z = k \cos \theta_1$ and $k_z = k \cos \theta_2$ ⁷. Since all resonances of the Airy function have equal area (in the limit $R_1/R_2 \rightarrow 1$), equal fractions of emission couple to each of the cavity modes. Therefore in the case of sharp, well-separated resonances the extraction efficiency η_{extra} becomes

$$\eta_{extra} = \frac{\text{number of modes with } \theta < \theta_c}{\text{total number of modes}} \quad (2)$$

In the large cavity limit illustrated in Figure 4(a), because the $\cos \theta$'s of the large number of cavity modes are equally spaced from 1 to 0, this ratio tends towards the ratio (solid angles $< \theta = \theta_c$)/ $2\pi = 1 - \cos \theta_c \approx 1/2n^2$. This is the same extraction efficiency expected for a single bottom mirror far from the source. However if we consider the microcavity regime as illustrated in Figure 4(b), when there are only a few cavity modes and specifically only one at $\theta < \theta_c$, then

$$\eta_{extra} = \frac{1}{m_c} \quad (3)$$

giving $\eta_{extra} = 0.25$ for the situation illustrated in Figure 4(b). Ultimately we could imagine a $\eta_{extra} = 1$ value for a cavity with only a single mode whose Airy resonance was confined to angles $\theta < \theta_c$, however as discussed below such a cavity is beyond the limits of current technology.

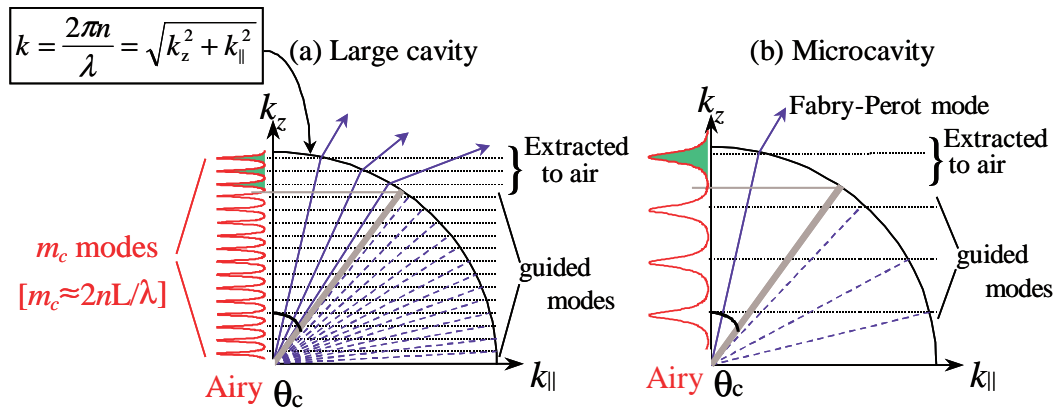


Figure 4 Plot in k-space depicting cavity modes, air function and critical angle. The shaded area under the Airy function at $\theta < \theta_c$ is proportional to the extracted emission. (a) large cavity limit – many modes extracted (b) microcavity regime – one of a small number of modes extracted.

At this stage we can re-introduce the antinode factor ζ_i , to allow the possibility of different coupling between the source and the different cavity modes due to the source location or orientation. If we label each cavity mode $i=1,2,\dots,m_c$, then we can assign each mode an antinode factor ζ_i (assuming sharply defined resonances allow the identification of a single ζ_i for each mode). Then we can rewrite a corrected form of the generalized expression (2) as

$$\eta_{extra} = \frac{\sum_{\text{extracted modes}} \zeta_i}{\sum_{\text{all modes}} \zeta_i} \quad (4)$$

which becomes

$$\eta_{extra} = \frac{\zeta}{\sum_{\text{all modes}} \zeta_i} \quad (5)$$

for the microcavity case with a single extracted mode of antinode factor ζ .

This treatment of the ability of a planar microcavity structure to alter the emission pattern and extraction efficiency of an isotropic emitter has not been extended to include important factors in practical structures such as the source emission linewidth, the angular dependence of mirror reflectivities, and the distributed nature of reflections from certain mirrors. However it does highlight some important generic design considerations/operating principles of RCLED structures:

1. The positioning of the source at the antinode (node) of a cavity mode to enhance (inhibit) emission into that mode.
2. The importance of minimizing the cavity length, which determines the total number of cavity modes, in order to maximize the fraction of emission coupled to the extracted mode of the cavity.

2.2 Details of model

In order to accurately model the performance of practical RCLED devices incorporating DBR and metallic mirrors a numerical simulation tool capable of the exact calculation of dipole emission modifications in an arbitrary multilayer structure was implemented. The modeling tool was initially developed to simulate the performance of RCLEDs emitting at 980nm⁹ and is capable of calculating the enhancement or inhibition of emission from the active layer of a cavity, due to the modified optical environment, as a function of angle and wavelength given the refractive index (real and imaginary) and thickness of each layer in the structure. Multiplication of the intrinsic emission spectrum of the active region (in the absence of any cavity effects) by the cavity enhancement factors at the corresponding wavelengths produces the RCLED emission as a function of wavelength and angle. Comparison of the total extracted emission (or the fraction that is emitted into air at angles less than $\sin^{-1}(\text{NA})$ for the extraction efficiency into a reduced NA) integrated over angles and wavelengths with the total internal emission from the active layer gives the extraction efficiency of the RCLED.

The details of the model are contained in reference 10. It is based on the transfer matrix technique for propagating electromagnetic waves of a given TE or TM polarization through a multilayered structure, with source terms introduced as an additive discontinuity to the electromagnetic field at the dipole (active) layer. The source terms are dependent on the polarization of the wave and the orientation of the emitting dipole with respect to the layer interfaces. The model deals purely with the optical properties of the cavity and takes no account of electrical issues such as carrier transport and leakage, and therefore provides no information about the injection or radiative efficiencies of the device.

The InGaN/GaN QW emission is modelled by a distribution of non-correlated isotropic dipoles, located at the centre of the QW layer. The refractive index values for $\text{Al}_x\text{Ga}_{1-x}\text{N}$ and InGaN were taken from the literature^{11,12} while refractive index values of the metal mirror were taken from spectroscopic ellipsometry measurements performed on a silver layer.

2.3 Design optimization procedure

Before performing the optimization procedure two device parameters are fixed by material growth considerations; the aluminum (Al) fraction in the AlGaIn/GaN DBR and the intrinsic emission linewidth (a Gaussian spectral lineshape is assumed) from the InGaIn/GaN QWs.

Once these two quantities are known there are three design parameters that have to be simultaneously optimized:

1. The thickness of the central cavity, which firstly determines the cavity order ($1\lambda, 3\lambda/2, 2\lambda\dots$). Small adjustments to the thickness of the cavity adjust the angle of the cavity mode resonance for a fixed cavity order. Detailed calculations have shown that the maximum extraction efficiency into air ($\text{NA}=1$) occurs when the peak QW emission wavelength is resonantly extracted off-axis. The angular dispersion of the cavity mode results in QW emission at wavelengths shorter (longer) than the peak QW emission wavelength being resonantly extracted at larger (smaller) angles. A consequence of the positioning of the cavity mode to achieve maximum efficiency into air ($\text{NA}=1$) is a two lobed farfield emission pattern, which is undesirable for maximum emission efficiency into a reduced NA. Therefore the optimum cavity thickness for maximum extraction efficiency is dependent on the NA into which emission is considered.
2. The number of DBR pairs, which determines the reflectivity of the DBR mirror. Adjusting the reflectivity of the DBR mirror adjusts the cavity mode linewidth, which determines the range of wavelengths/angles over which emission is enhanced.
3. The position of the QWs in the cavity. The magnitude of the E-field of the extracted mode at the location of the QWs determines the coupling of emission to the extracted mode. Positioning the QW layer at an antinode of the extracted mode results in a factor of two increase in extraction efficiency over a distributed source throughout the cavity⁷.

In order to optimize these three parameters, the performance of RCLEDs with a range of numbers of DBR pairs is modeled. For each number of DBR pairs the extraction efficiency is calculated at a range of cavity thicknesses, with the QW positioned at the max of the calculated E-field of the extracted mode at each step.

3. RESULTS AND DISCUSSION

3.1 Optimized RCLED design and performance for maximum extraction efficiency

In this section the optimum extraction efficiencies into NAs of 1.0 and 0.5 that can be achieved by a metal-DBR GaN RCLED emitting at 510nm, and the corresponding designs are presented. The optimization was performed for a range of Al fractions in the DBR (between 0 and 1, step 0.1) and QW emission linewidths (between 16nm and 40nm). A central cavity thickness of $\approx 5\lambda/4$ (thickness was adjusted to optimize angle of cavity mode resonance, but not cavity order) was used in all cases. The active region consisted of 3 InGaN/GaN QWs positioned at the central antinode of the extracted mode throughout. Emission from the three QWs was modeled by a single dipole layer positioned at the center of the central QW in our structure. This approximation to the physical situation where emission occurs from all three QWs in our structure, only introduces a small correction to our calculated results due to the close spacing of the QWs (the correction factor to the calculated efficiencies is estimated between 0.9-1.0 from Figure 7).

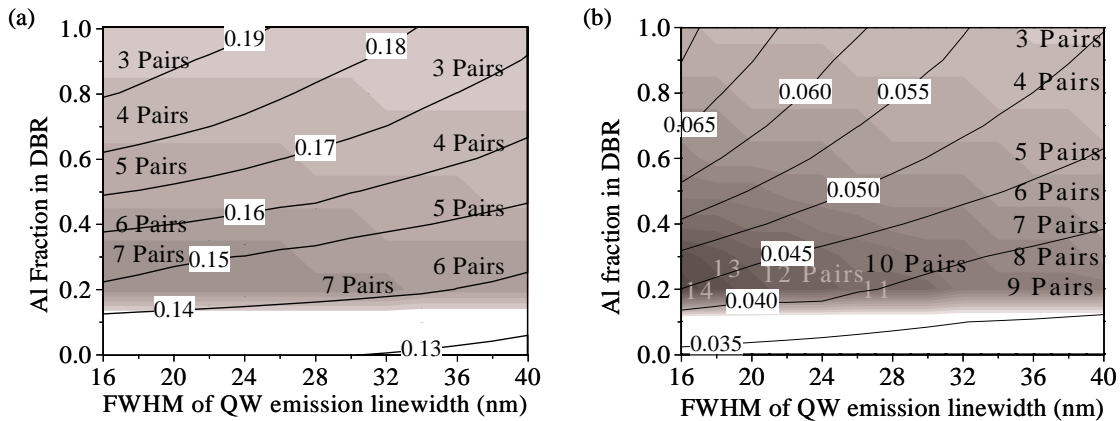


Figure 5. Contour plots of maximum extraction efficiency (lines) and corresponding number of DBR pairs (shading) as functions of Al fraction in DBR and QW emission linewidth for emission into (a) NA=1.0 and (b) NA=0.5. (the optimum number of DBR pairs is not shown for Al fractions <0.15 due to the extremely small variation in efficiency with number of DBR pairs)

The optimized device designs and the corresponding extraction efficiencies are shown in Figure 5. A decrease in extraction efficiency with increasing QW linewidth and decreasing Al fraction is observed for both emission NAs considered. The angular dispersion of the cavity mode wavelength allows the cavity to be designed for maximum extraction efficiency of only a single emission wavelength, resulting in a decrease in the extraction efficiency obtainable as the QW emission linewidth increases. The decrease in extraction efficiency with decreasing Al fraction in the DBR is due to the reduction in the refractive index contrast between alternate layers in the DBR. This reduced refractive index contrast results in a reduced DBR reflectivity stopband and an increased penetration depth of the light into the DBR, which increases the effective cavity length. Both these effects limit the ability of the cavity to enhance the extraction efficiency.

The optimum number of DBR pairs is observed to decrease with increasing QW linewidth and increasing Al fraction. These trends can be understood qualitatively in terms of the role the cavity mode spectral linewidth plays in determining the extraction efficiency. A narrow cavity mode spectral linewidth results in a strong enhancement of a small range of wavelengths, while a wider cavity mode linewidth results in a weaker enhancement of a broader range of wavelengths. As the intrinsic QW emission linewidth increases a broader cavity mode linewidth is required to enhance a wider range of source emission wavelengths. A reduction in the number of DBR pairs and hence a decrease in the DBR mirror reflectivity produces such an increase in the cavity linewidth. Correspondingly at a fixed QW emission linewidth an increase in the Al fraction in the DBR requires a reduction in the number of DBR pairs in order to maintain this reflectivity.

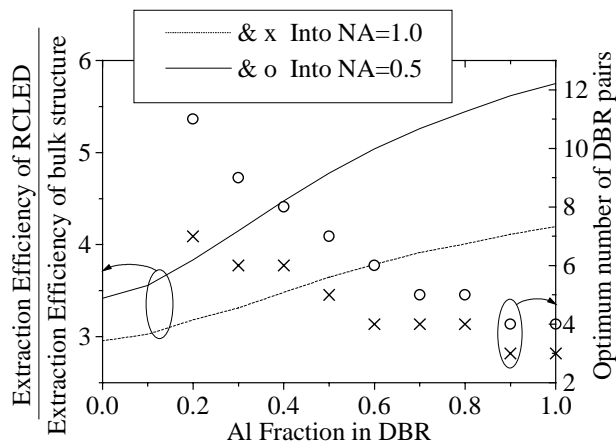


Figure 6 Comparison of efficiency enhancement factors and optimum numbers of DBR pairs for emission into NA=1.0 and NA=0.5, assuming a QW emission linewidth of 30nm.

In Figure 6 the maximum extraction efficiencies and optimum numbers of DBR pairs for emission into NAs of 1.0 and 0.5 assuming a typical InGaN/GaN QW emission linewidth of 30nm¹³ are compared. The extraction efficiencies are plotted as multiples of the corresponding extraction efficiencies of a conventional bulk LED structure emitting through a single facet (same structure as shown in Figure 1 but with the mirrors removed and thick cavity spacer layers). Even for the single mirror structure (i.e. silver metal mirror only, Al fraction in DBR = 0) enhancement factors of 3.0 and 3.4 of the extraction efficiencies are predicted over the bulk LED structure. These single mirror efficiency enhancement factors are greater than the factor of two expected from a simple geometrical mirror effect due to the exploitation of constructive interference effects that come when a localized source is correctly positioned near a single mirror. The efficiency enhancement factors increase with increasing Al fraction in the DBR up to values of 4.2 and 5.8 for emission into NAs of 1 and 0.5 respectively for a metal-AlN/GaN DBR cavity structure. The enhancement of efficiency is greater for the NA=0.5 case due to the RCLEDs ability to enhance emission into a limited range of angles by reducing the angular width of the cavity mode resonance. The angular width of the cavity mode resonance for a single wavelength can be reduced by increasing the DBR mirror reflectivity, explaining the greater number of DBR pairs in the optimum RCLED design for maximum extraction efficiency into a NA of 0.5 compared to a NA of 1.

3.2 Critical design parameters

While AlN/GaN DBRs have been reported¹⁴, epitaxial growth considerations usually limit the Al fraction to between 0.25 and 0.4^{15,16}. In the light of this limitation the performance of a RCLED structure incorporating a 9 period Al_{0.3}Ga_{0.7}N/GaN DBR and a single QW active region was further investigated. The spacings between the metal mirror and QW, and the QW and DBR were simultaneously varied, and the extraction efficiency of the RCLED was calculated for each combination of spacings. The result of this simulation is shown in Figure 7. The extraction efficiency exhibits a periodic dependence on the thickness of both cavity spacer layers. The variation in efficiency is greater when moving vertically along the contour plot, which corresponds to varying the metal-QW spacing at a fixed DBR-QW spacing, than when moving horizontally through the plot, which corresponds to varying the DBR-QW spacing at a fixed metal-DBR spacing. Clearly the correct positioning of the QW with respect to the metal mirror is crucial to the performance of the RCLED.

The diagonal lines in Figure 7 represent structures with constant cavity thickness and hence resonant wavelength, with variations along a single diagonal caused by changes in the position of the active region in the cavity. The maxima (minima) along the diagonal correspond to the QW positioned at an antinode (node) of the cavity. The nearer the antinode at which the QW is placed is to the metal mirror the higher the efficiency.

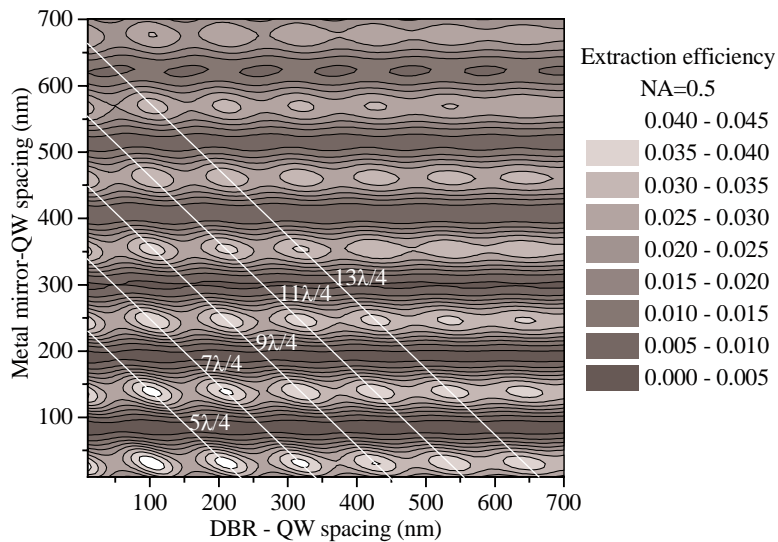


Figure 7. Contour plot of modeled extraction efficiency into NA=0.5 of metal- $\text{Al}_{0.3}\text{Ga}_{0.7}\text{N}/\text{GaN}$ DBR RCLED as functions of top and bottom cavity spacer layers, assuming a QW emission linewidth of 30nm. The diagonal white lines mark cavity structures with near optimum cavity resonance wavelength, labeled with the optical thickness of the central cavity region.

To illustrate the importance of correctly positioning the QW in the cavity, a comparison of the variation in extraction efficiency with QW position and total cavity thickness is shown in Figure 8. The extraction efficiency varies between 0.041 and 0.003 when varying the QW position in a cavity of optimal total thickness, while the minimum efficiency when varying the total cavity thickness while maintaining the QW at its optimal position in the cavity is 0.028 .

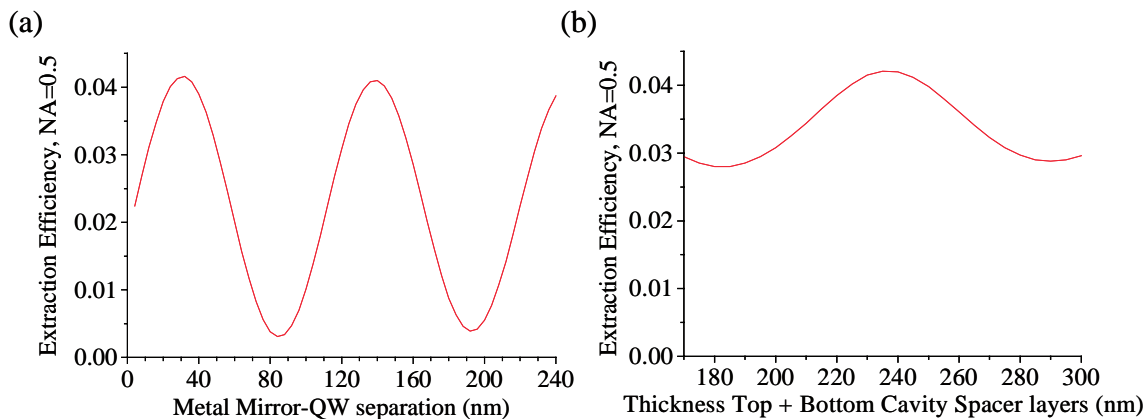


Figure 8. Variation in extraction efficiency of $5\lambda/4$ RCLED with (a) QW position cavity of optimal thickness and (b) central cavity thickness with QW optimally positioned.

3.3 Farfield emission patterns

The results presented in section 3.2 show that the position of the QW in the cavity, and specifically the spacing between the QW and the metal mirror, is critical to the performance of the RCLED device. Standard white light reflectivity measurements are often performed on RCLED structures to provide information on the cavity modal properties. The mirror reflectivities, the DBR spectral stopband, and the separation of the mirrors can be determined from reflectivity measurements. However it is very difficult to determine any information on the position of the QW active region in the cavity from reflectivity measurements. Therefore the variation in the farfield emission pattern with QW position in a RCLED device was simulated to investigate whether farfield measurements would provide a method for determining this important device parameter. The results of these simulations are shown in Figure 9. A strong variation in the shape of the farfield emission profile is predicted with QW position. When the QW is optimally positioned at an antinode of the cavity, the farfield emission pattern is approximately constant in the 0-25 degree angular range, and decreases at greater angles. In contrast the maximum in the farfield emission pattern occurs at an angle of 50 degrees from the normal when the QW is positioned at a node of the cavity. Therefore farfield measurements should provide valuable information on the position of the QW in the RCLED.

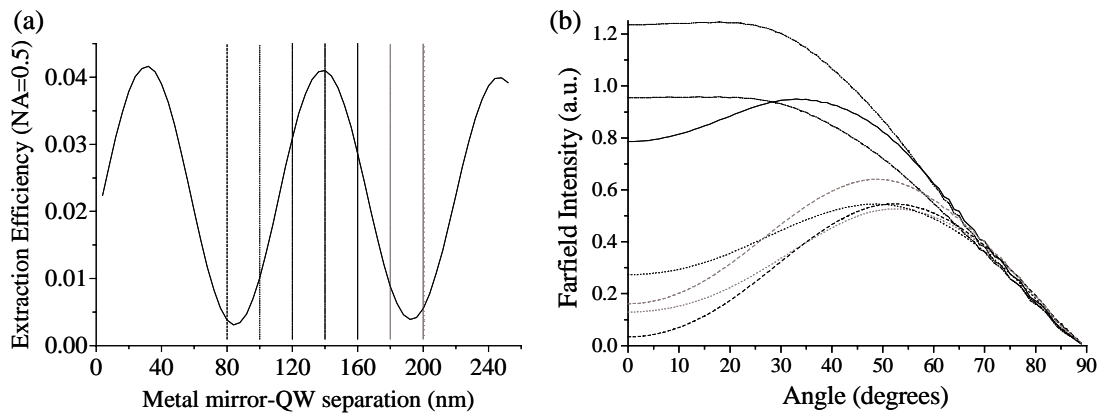


Figure 9. (a) Extraction efficiency of $5\lambda/4$ RCLED with QW position in the cavity (cavity length fixed at optimum value for maximum efficiency, bottom DBR was a 5 period $\text{Al}_{0.3}\text{Ga}_{0.7}\text{N}/\text{GaN}$ structure). (b) The simulated farfields for metal mirror-active region separations indicated by the coded vertical lines in graph (a).

3.4 Emission linewidth calculations

In a RCLED the cavity enhances emission from the QW matched to the cavity mode. At a discrete angle the range of wavelengths at which emission is enhanced is determined by the cavity mode linewidth. Therefore adjusting the mirror reflectivities can control the spectral emission linewidth from the RCLED at a discrete angle. However the cavity mode shifts with angle resulting in the enhancement of different emission wavelengths at different angles. Therefore reducing the cavity mode linewidth at a single angle does not guarantee a reduction in the spectral linewidth of the angle-integrated emission. The role of mirror reflectivities and source emission linewidth play in determining the RCLED emission linewidth are extensively discussed in reference 7.

Simulations of the emission spectrum from our metal-DBR GaN RCLED structure, assuming an intrinsic QW emission linewidth of 30nm, show only a small reduction of the angle integrated emission linewidth for emission into an NA of 1.0, even for large numbers of DBR pairs. However when considering emission into a reduced NA, significant narrowing of the spectral is predicted as shown in Figure 10(a). The emission linewidth decreases with increasing number of DBR pairs from 27nm for a single metal mirror device and reaching a lower limit of 12nm at large number of DBR pairs. The number of DBR pairs required to reach this lower limit increases with decreasing Al fraction in the DBR. Comparison of the calculated emission linewidths and extraction efficiencies in Figure 10(a) and 10(b) respectively, shows that the number of DBR pairs required to obtain the minimum spectral emission linewidth is greater than the optimum number of pairs for maximum extraction efficiency. Therefore the minimum emission linewidth can only be obtained at a reduced efficiency.

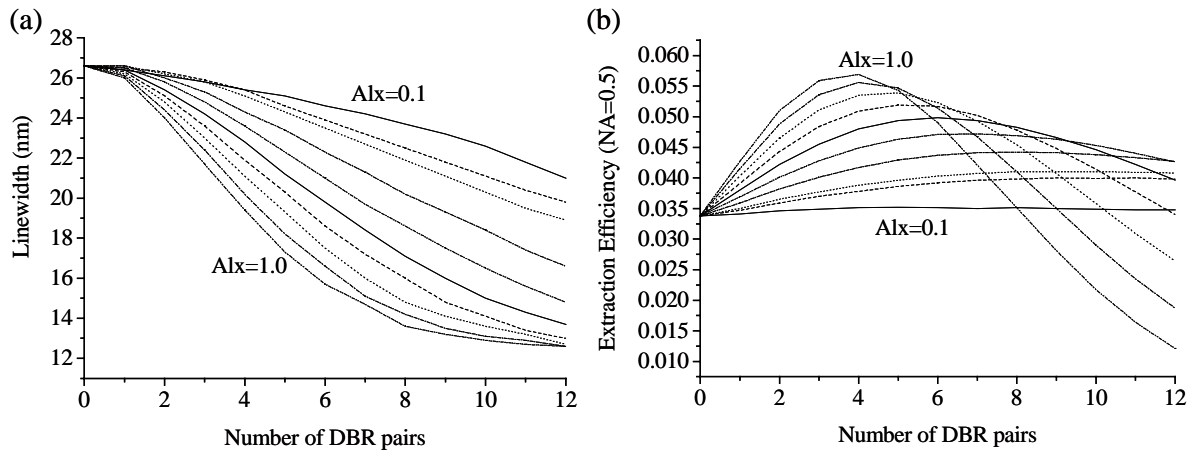


Figure 10. (a) Spectral linewidth of RCLED emission into a reduced NA of 0.5. The spectral linewidth is plotted for GaN RCLEDs with Al fractions in the AlGaN/GaN DBR between 0.1 and 1.0. (b) The extraction efficiency into an NA of 0.5 for the same RCLED devices as in (a).

4. CONCLUSIONS

The enhancement of emission from an internal source into the modes of a cavity can be used to produce RCLEDs with increased extraction efficiency compared to conventional LEDs. Using a model based on the transfer matrix method the emission properties of a GaN RCLED have been investigated. The RCLED design has been optimized for maximum extraction efficiency into NAs of 1 (total emission) and 0.5 (typical POF NA), for a range of Al fractions in the DBR and QW emission linewidths. The maximum predicted extraction efficiency for a RCLED incorporating a AlN/GaN DBR, assuming a 30nm QW emission linewidth, is 0.18 (0.055) into an emission NA of 1.0 (0.5). The Al fraction in the DBR is currently typically limited by growth considerations to 0.3, in which case the optimized extraction efficiency is 0.15 (0.04) into an emission NA of 1.0 (0.5). The number of DBR pairs in the optimized RCLED design varies between 3 and 13, depending on the Al fraction in the DBR, the QW emission linewidth, and the emission NA considered. The corresponding optimized DBR reflectivity varies between 0.05 and 0.50.

The spacing between the QW active layer and the metal mirror is shown to be the crucial design parameter in determining the extraction efficiency of our RCLED incorporating an Al_{0.3}Ga_{0.7}N/GaN DBR. The reduction in efficiency for non-optimal placement of the QW in the cavity is greater than for a non-optimal total cavity thickness. The variation in the farfield emission pattern of the RCLED with the QW-metal mirror spacing should provide a method of determining this crucial device parameter. It has also been shown that coupling of the RCLED emission into a reduced NA of 0.5 results in significant reduction of the spectral linewidth. The spectral linewidth into a NA of 0.5 decreases towards a lower limit with increasing number of DBR pairs in the RCLED, with the number of DBR pairs required to produce the minimum emission linewidth greater than the optimal number for maximum extraction efficiency.

The optical properties of the metal-DBR GaN RCLEDs suggest the devices are promising sources for POF applications. The modeling results highlight the ability of the cavity to enhance the extraction efficiency compared to conventional LED structures, especially into a reduced NA. While the efficiency enhancement factors compared to non-cavity devices of the GaN RCLEDs are less than for red GaInP RCLEDs, the absolute efficiencies of the RCLEDs are similar at the two wavelengths. Therefore in the case of similar internal efficiencies in both devices, the overall efficiencies of both green and red RCLEDs would be similar, with the green GaN RCLED offering the potentially important advantage of improved temperature characteristics.

ACKNOWLEDGEMENTS

This research was funded by the European IST program AGETHA 1999-10292.

REFERENCES

- ¹ E. F. Schubert, Y.-H. Wang, A. Y. Cho, L.-W. Tu, and G. J. Zydzik, "Resonant cavity light-emitting diode", *Appl. Phys. Lett.* **60**, pp. 921-923, 1992.
- ² H. De Neve, J. Blondelle, P. Van Daele, P. Demeester and R. Baets, "Recycling of guided mode light emission in planar microcavity light emitting diodes", *Appl. Phys. Lett.* **70**, 799-801, 1997
- ³ R. Wirth, C. Karnutsch, S. Kugler, and K. Streubel, "High-Efficiency Resonant-Cavity LEDs Emitting at 650nm" *IEEE Photon. Technol. Lett.* **13**, pp. 421-423, 2001
- ⁴ Y.-K. Song, M. Diagne, H. Zhou, A. V. Nurmikko, R. P. Schneider, Jr. and T. Takeuchi, "Resonant-cavity InGaN quantum-well blue light-emitting diodes", *Appl. Phys. Lett.* **77**, pp. 1744-1746, 2000.
- ⁵ M. Diagne, Yiping He, H. Zhou, E. Makarona, A. V. Nurmikko, J. Han, T. Takeuchi, and M. Krames, "A High Injection Resonant Cavity Violet Light Emitting Diode Incorporating (Al,Ga)N Distributed Bragg Reflector" *phys. stat. sol. (a)* **188**, pp. 105-108, 2001.
- ⁶ H. Benisty, "Physics of Light Extraction Efficiency in Planar Microcavity Light-Emitting Diodes", *Confined Photon Systems – Fundamentals and Applications*, H. Benisty, J.-M. Gérard, R. Houdré, J. Rarity, and C. Weisbuch, pp. 393-405, Springer, Berlin, 1999.
- ⁷ H. Benisty, H. De Neve, C. Weisbuch, "Impact of planar microcavity effects on light extraction: I. Basic concepts and analytical trends", *IEEE J. Quantum Electron.* **34**, pp. 1612-1631, 1998.
- ⁸ H. Benisty, H. De Neve, C. Weisbuch, "Impact of planar microcavity effects on light extraction: II. Selected exact simulations and role of photon recycling", *IEEE J. Quantum Electron.* **34**, pp. 1632-1643, 1998.
- ⁹ Reports of EC ESPRIT #8447, Semiconductor Microcavity Light Emitters (SMILES) project, 1993-1997.
- ¹⁰ H. Benisty, R. Stanley, and M. Mayer, "Method of source terms for dipole emission modification in modes of arbitrary planar structures", *J. Opt. Soc. Am. A* **15** (5) pp. 1192-1201, 1998.
- ¹¹ G. M. Laws, E. C. Larkins, I. Harrison, C. Molloy, and D. Somerford, "Improved refractive index formulas for the $\text{Al}_x\text{Ga}_{1-x}\text{N}$ and $\text{In}_y\text{Ga}_{1-y}\text{N}$ alloys" *J. Appl. Phys.* **89**, pp. 1108-1115, 2001.
- ¹² M. M. Y. Leung, A. B. Djurišić and E. H. Li, "Refractive index of InGaN/GaN quantum well", *J. Appl. Phys.* **84**, pp. 6312-6317, 1998.
- ¹³ S. Nagahama, N. Iwasa, M. Senoh, T. Matsushita, Y. Sugimoto, H. Kiyoku, T. Kozaki, M. Sano, H. Matsumura, H. Umemoto, K. Chocho, T. Yanamoto, and T. Mukai, "GaN-Based Light-Emitting Diodes and Laser Diodes, and Their Recent Progress", *phys. stat. sol. (a)*, **188**, pp. 1-7, 2001.
- ¹⁴ H. M. Ng, T. D. Moustakas, and S. N. G. Chu, "High reflectivity and broad bandwidth AlN/GaN distributed Bragg reflectors grown by molecular-beam epitaxy", *Appl. Phys. Lett.* **76**, pp. 2818-2820, 2000.
- ¹⁵ T. Someya and Y. Arakawa, "Highly reflective GaN/Al_{0.34}Ga_{0.66}N quarter-wav reflectors grown by metal organic chemical vapor deposition" *Appl. Phys. Lett.* **73**, pp. 3653-3655, 1998.
- ¹⁶ N. Nakada, M. Nakaji, H. Ishikawa, T. Egawa, M. Umeno, and T. Jimbo, "Improved characteristics of InGaN multiple-quantum-well light-emitting diode by GaN/AlGaN distributed Bragg reflector grown on sapphire" *Appl. Phys. Lett.* **76**, pp. 1804-1806, 2000.